



IJRASET

International Journal For Research in
Applied Science and Engineering Technology



INTERNATIONAL JOURNAL FOR RESEARCH

IN APPLIED SCIENCE & ENGINEERING TECHNOLOGY

Volume: 13 **Issue:** IV **Month of publication:** April 2025

DOI: <https://doi.org/10.22214/ijraset.2025.66837>

www.ijraset.com

Call:  08813907089

E-mail ID: ijraset@gmail.com

Design and Controlled for Bridgeless Zeta-Luo Converter for EV Charging

Vishal Kardak¹, Roshan Bodke², Chandan Dhake³, Umesh Kalyankar⁴

Abstract: *The widespread adoption of electric vehicles (EVs) has necessitated the development of efficient and reliable charging infrastructure. Conventional EV chargers often employ bridge rectifiers, which can lead to significant conduction losses due to the presence of high-voltage diodes. To address this limitation, a novel EV charger based on a bridgeless (BL) isolated Zeta-Luo converter with built-in power factor (PF) preregulation capability at the supply side has been proposed. The BL isolated Zeta-Luo converter is a combination of a Zeta converter and a Luo converter, each operating during alternate halves of the supply voltage cycle. This approach eliminates the need for bridge rectifiers, reducing conduction losses and improving overall efficiency. Additionally, the shared output inductors of the Zeta and Luo converters further contribute to the compact size and lightweight design of the charger. The built-in PF preregulation capability ensures that the charger operates with a near-unity power factor, minimizing reactive power consumption and improving grid stability. This is achieved by regulating the input current waveform to closely match the input voltage waveform. The proposed EV charger offers several advantages over conventional chargers, including:*

The BL topology and shared output inductors significantly reduce semiconductor losses, leading to improved efficiency. The built-in PF Preregulation capability ensures near-unity power factor operation, minimizing reactive power consumption and improving grid stability. The elimination of bridge rectifiers and the sharing of output inductors result in a compact and lightweight charger design. Enhanced performance under sudden voltage variations: The proposed charger exhibits robust performance under sudden line voltage fluctuations, ensuring reliable EV charging even during unstable grid conditions. The Bridgeless Isolated Zeta-Luo Converter-Based EV Charger With PF Preregulation presents a promising solution for efficient and reliable EV charging. Its combination of high efficiency, improved power factor, reduced size, and enhanced performance under voltage variations makes it an attractive choice for future EV charging infrastructure.

Keywords: *Power Factor Correction, Zeta-Luo Converter, FLC Controller, EV Charging, DCM*

Abbreviations

BEV	Battery-based Electric Vehicle Power
PQ	Quality
DBR	Diode Bridge Rectifier Power
PFP	Factor Preregulator
EMI	Electromagnetic Interference
PFC	Power Factor Correction
EV	Electric Vehicle
CC	Constant Current
CV	Constant Voltage
THD	Total Harmonic Distortion
IIC	Inductor-Inductor Capacitor
MOSFET	Metal-oxide-semiconductor field-effect transistor Pulse
PWM HFT	Width Modulation
SoC	High Frequency Transformer State of Charge

List of Figures

- Figure1.1 CircuitdiagramofZETA converter
- Figure1.1 ZETAconverterduringCCMoperation
- Figure1.3 ZETAconverter’s componentcurrentsduringCCM
- Figure1.4 CircuitdiagramofZETA converter
- Figure1.5 CircuitDiagramforMode1
- Figure1.6 CircuitDiagramforMode2
- Figure1.7 ZETAconverter’s componentcurrentsduringDCM
- Figure2.1 Circuitconfigurationof IsolatedZetaconverter
- Figure2.2 CircuitconfigurationofIsolatedLuoconverter
- Figure2.3 CircuitconfigurationofBLisolatedZeta–Luoconverter-basedcharger.
- Figure3.1 OperationofZeta–Luoconverter forthreeswitching statesMode-IZeta mode
- Figure3.2 OperationofZeta–Luo converterforthreeswitchingstates Mode-IIZeta mo
- Figure3.3 OperationofZeta–Luoconverterfor threeswitchingstatesMode-IIIZetamode
- Figure3.4 Charginganddischargingsequenceofdifferentcomponentsoveraswitching cycleforZeta andLuomodes.
- Figure3.5 OperationofZeta–LuoconverterforthreeswitchingstatesMode-ILuo mode (-vehalfline).
- Figure3.6 OperationofZeta–LuoconverterforthreeswitchingstatesMode-IIILuomode(-vehalfline).
- Figure3.7 OperationofZeta–LuoconverterforthreeswitchingstatesMode-IIILuo mode(-vehalfline).

- Figure5.1 CircuitDiagramforZeta-Luo Converter
- Figure5.2 PowerFactor Waveform
- Figure5.3 InputACVoltageandCurrentwaveform
- Figure5.4 InductorVoltageWaveform
- Figure5.5 DC Output VoltageWaveform
- Figure5.6 BatteryVoltageWaveform
- Figure5.7 DCLoadCurrentWaveforms Waveform

Symbols and Notations

I_{dcref}	Referencecurrent
V_{dcre}	ReferenceVoltage
f	
V_{spk}	rmssource voltage
ω	Supply Frequency
Δ	Depictstherippleinconverterdc-link voltage
θ	Angleby linecurrentleads or lags
Υ	Voltage Ripple
K_{pv}	ProportionalgainconstantforVoltage
K_{iv}	Integralgain constantfor Voltage
V_{dc}	Output DC Voltage
I_{dc}	Output DC Current

C_f	FilterCapacitor
C_{dc}	CapacitorDC Voltage
L_f	Filter Inductor
V_s	Supply Voltage
L_{m1}	MagnetizingInductance
S_1	Switch1
S_2	Switch2
I_s	Supply Current
I_{l0}	InductorCurrent
F_{cr}	FilterCut-Frequency

I. INTRODUCTION OF ZETA AND LUO CONVERTER

A. Introduction

Introduction Similar to the SEPIC DC/DC converter topology, the ZETA converter topology provides a positive output voltage from an input voltage that varies above and below the output voltage. The ZETA converter also needs two inductors and a series capacitor, sometimes called a flying capacitor. Unlike the SEPIC converter, which is configured with a standard boost converter, the ZETA converter is configured from a buck controller that drives a high-side PMOS FET. The ZETA converter is another option for regulating an unregulated input-power supply, like a low-cost wall wart. To minimize board space, a coupled inductor can be used. This article explains how to design a ZETA converter running in continuous-conduction mode (CCM) with a coupled inductor.

B. Circuit Diagram of Zeta Converter

The below figure shows the schematic diagram of a zeta converter. It consists of two inductors, a capacitor, and a diode. The circuit of the zeta converter is almost similar to a single-ended primary-inductor converter (SEPIC) except in the place of the diode in SEPIC, there is an inductor in the zeta converter, and in the place of these second inductor in SEPIC, there is a diode in zeta converter.

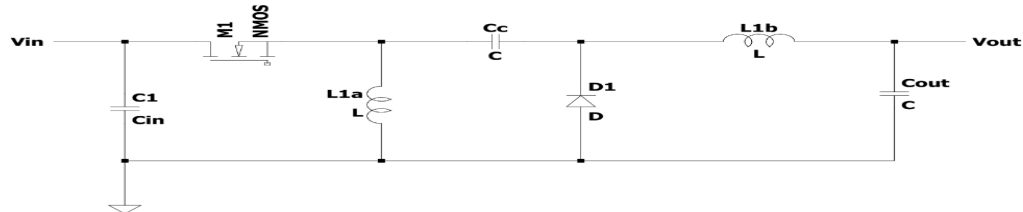


Fig.1.1 Circuit diagram of ZETA converter

The capacitor C_1 acts as the bridge between the input and output sides of the converter. It also isolates input and output sides from each other. Generally, a transistor (MOSFET or IGBT or BJT) is used as the switch in dc-to-dc converters, due to low power loss, higher input impedance, and simple driver circuitry MOSFETs are mostly used.

The MOSFET switching is controlled by PWM pulses applied at the gate terminal and feedback taken from the output so that the desired regulated output will be obtained.

C. Working of Zeta Converter

Figure 1.1 shows a simple circuit diagram of a ZETA converter, consisting of an input capacitor, C_{IN} ; an output capacitor, C_{OUT} ; coupled inductors L_{1a} and L_{1b} ; an AC coupling capacitor, CC ; a power PMOS FET, Q_1 ; and a diode, D_1 . Figure 2 shows the ZETA converter operating in CCM when Q_1 is on and when Q_1 is off.

To understand the voltages at the various circuit nodes, it is important to analyze the circuit at DC when both switches are off and not switching. Capacitor CC will be in parallel with C_{OUT} , so CC is charged to the output voltage, V_{OUT} , during steady-state CCM. Figure 2 shows the voltages across L_{1a} and L_{1b} during CCM operation.

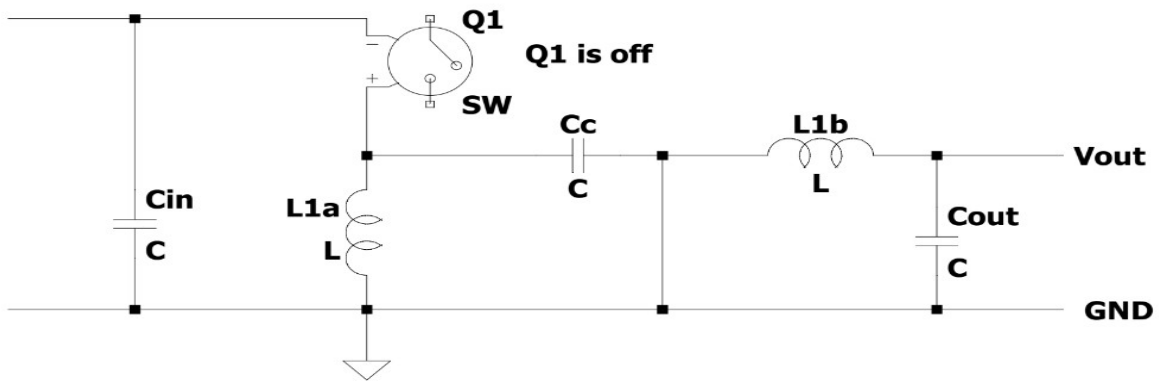


Figure.1.2ZETAconverterduringCCMoperation,whenQ1isOff

Mode1 [$t_0 - t_1$]: When Q_1 is off, the voltage across L_{1b} must be V_{OUT} since it is in parallel with C_{OUT} . Since C_{OUT} is charged to V_{OUT} , the voltage across Q_1 when Q_1 is off is $V_{IN} + V_{OUT}$; therefore, the voltage across L_{1a} is $-V_{OUT}$ relative to the drain of Q_1 . When Q_1 is on, capacitor C_c , charged to V_{OUT} , is connected in series with L_{1b} ; so the voltage across L_{1b} is $+V_{IN}$, and diode D_1 sees $V_{IN} + V_{OUT}$. The currents flowing through various circuit components are shown in Figure.1.2.

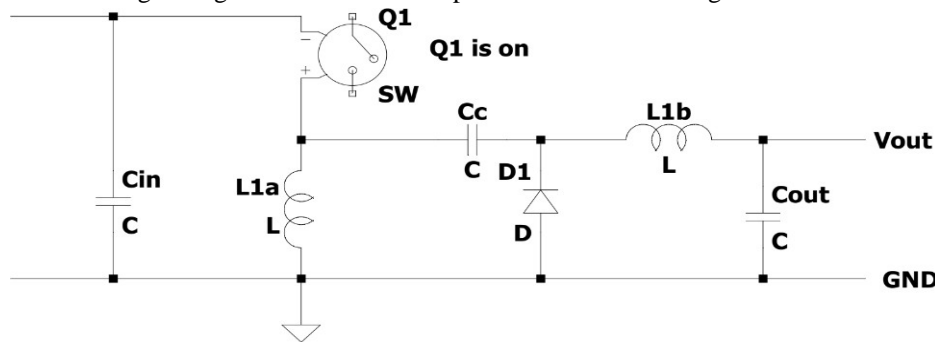


Figure1.3ZETAconverterduring CCM operation,whenQ1is on

Mode2 [$t_1 - t_2$]: When Q_1 is on, energy from the input supply is being stored in L_{1a} , L_{1b} , and C_c . L_{1b} also provides I_{OUT} . When Q_1 turns off, L_{1a} 's current continues to flow from current provided by C_c , and L_{1b} again provides I_{OUT} . The currents flowing through various circuit components are shown in Figure 1.3.

D. Introduction of LUO Converter (boost converter)

The Isolated DC-DC converters are commonly utilized for high power application because of high efficiency, simple control, steady state input current, high voltage gain and lower order voltage ripple contents. In recent days, many researchers have focussed on Luo converter due to high output voltage gain and continuous input current operation. This proposed converter is developed from Super lift elementary Luo converter topology. The PV application also requires high gain converters with optimized algorithms for tracking maximum power from input side. The boost converters are widely used in researches. The output voltage gain is very low for a boost and buck-boost converter topologies and it also has higher order ripple contents in its output voltage and thus the buck-boost type converter suffers from output voltage polarity problem. This drawback reduces the effectiveness of the converter. Buck-boost converter voltage is a non-isolated voltage. These drawbacks are overcome in . The isolated boost integrated converter is developed even though the gain is very less for this converter. To reduce the leakage reactance problem, magnetically coupled DC-DC converter is developed. This converter having high efficiency, the different shaped inductors reduce the leakage reactance problem. Finally Luo converter is developed to achieve high output gain with lifting constant all the existing issues are overcome. The proposed hybrid-lift DC-DC converter increases the output voltage gain with less ripple content. The PI controller achieves steady state voltage operation.

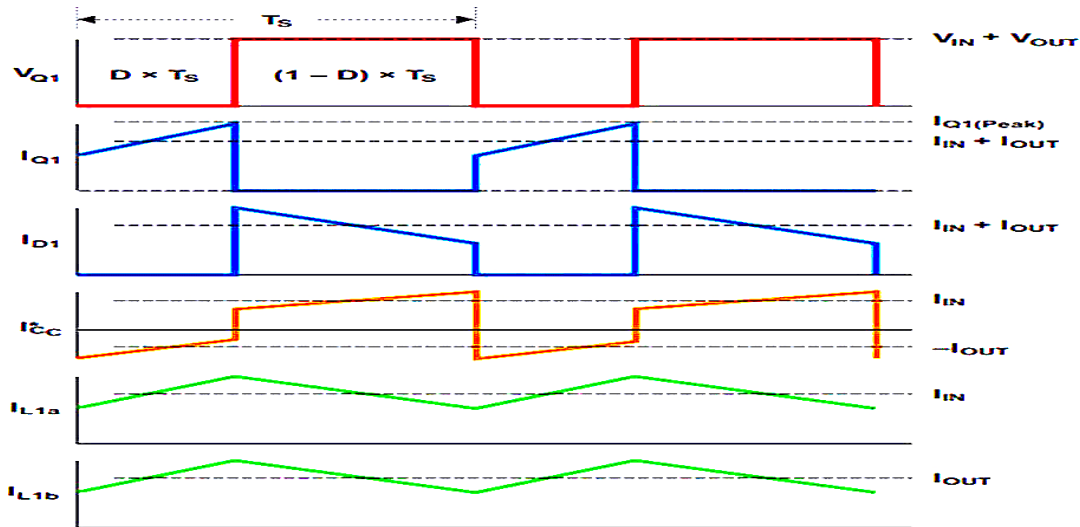


Fig.1.3,ZETAconverter'scomponentcurrentsduringCCM

E. Introduction of LUO Converter(boostconverter)

The Isolated DC-DC converters are commonly utilized for high power application because of high efficiency, simple control, steady state input current, high voltage gain and lower order voltage ripple contents. In recent days, many researchers have focussed on Luo converter due to high output voltage gain and continuous input current operation. This proposed converter is developed from Super lift elementary Luo converter topology. The PV application also requires high gain converters with optimized algorithms for tracking maximum power from input side. The

boost converters are widely used in researches. The output voltage gain is very low for a boost and buck-boost converter topologies and it also has higher order ripple contents in its output voltage and thus the buck-boost type converter suffers from output voltage polarity problem. This drawback reduces the effectiveness of the converter. Buck-boost converter voltage is a non-isolated voltage. These drawbacks are overcome in . The isolated boost integrated converter is developed even though the gain is very less for this converter. To reduce the leakage reactance problem, magnetically coupled DC-DC converter is developed. This converter having high efficiency, the different shaped inductors reduce the leakage reactance problem. Finally Luo converter is developed to achieve high output gain with lifting constant all the existing issues are overcome.

The proposed hybrid-lift DC-DC converter increases the output voltage gain with less ripple content. The PI controller achieves steady state voltage operation.

F. Working of Luo Converter

To analyze the operation of the Luo converter, the circuit can be divided into two modes. When the switch is ON, the inductor L_1 is charged by the supply voltage E . At the same time, the inductor L_2 absorbs the energy from source and the capacitor C_1 .

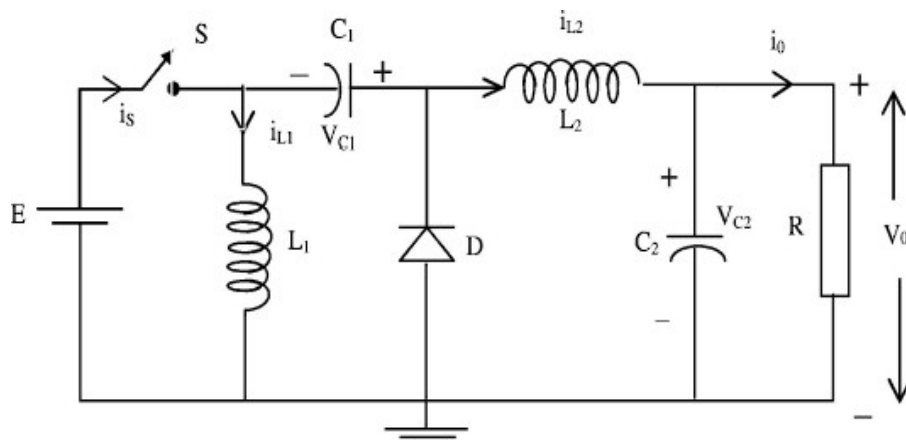


Figure.1.4,Circuit diagram of ZETA converter

The load is supplied by the capacitor C_2 . The equivalent circuit of Luo converter in mode 1 operation is shown in Figure.1.4. During switch is in OFF state, and hence, the current is drawn from the source becomes zero, as shown in Fig.1.5. Current i_{L2} flows through the freewheeling diode to charge the capacitor C_1 . Current i_{L2} flows through C_2-R circuit and the freewheeling diode D to keep itself continuous. If adding additional filter components like inductor and capacitor to reduce the harmonic levels of the output voltage.

Mode 1 [$t_0 - t_1$]: when the switch is ON, the inductor L_1 is charged by the supply voltage E . At the same time, the inductor L_2 absorbs the energy from source and the capacitor C_1 . The load is supplied by the capacitor C_2 . The equivalent circuit of Luo converter in mode 1 operation is shown in Figure.1.5

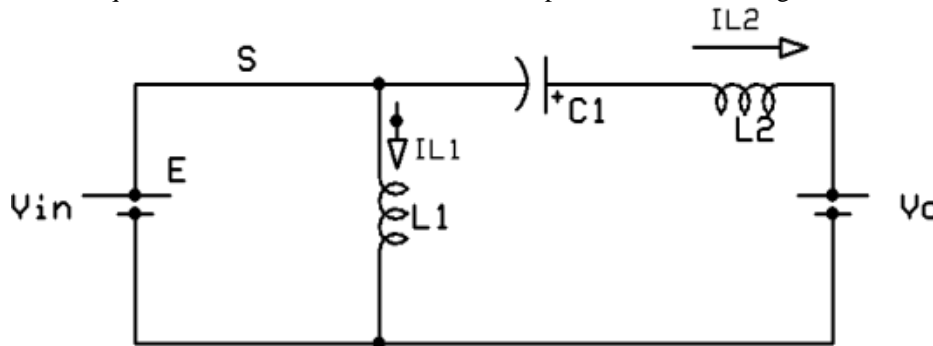


Fig. 1.5, Circuit Diagram for Mode 1

Mode 2 [$t_1 - t_2$]: switch is in OFF state, and hence, the current is drawn from the source becomes zero, as shown in (b). Current i_{L1} flows through the freewheeling diode to charge the capacitor C_1 . Current i_{L2} flows through C_2-R circuit and the freewheeling diode D to keep itself continuous operation is shown in Figure.1.6.

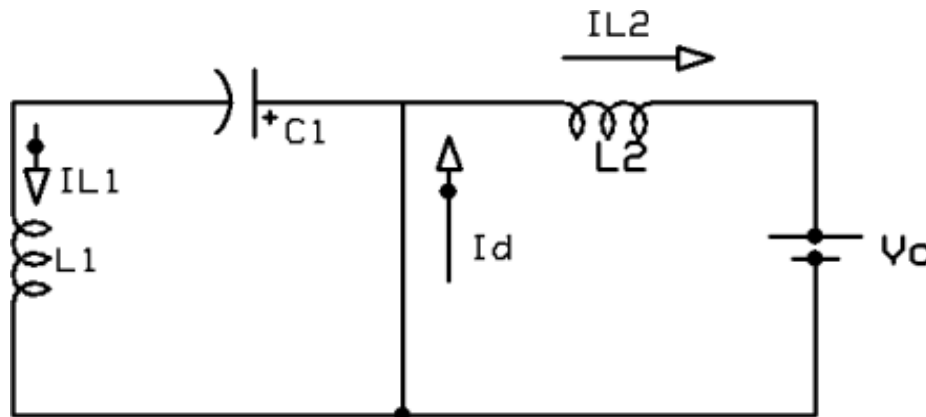


Figure. 1.6, Circuit Diagram for Mode 2

In discontinuous conduction mode, output should be in the form of discontinuous. In this mode diode is not present and inductor discharge through V_0 and L_2 . The output stage of the Luo buck converter is comprised of an inductor and capacitor. The output stage stores and delivers energy to the load, and smooths out the switch node voltage to produce a constant output voltage. Inductor selection directly influences the amount of current ripple seen on the inductor current, as well as the current capability of the buck converter itself. Inductors vary from manufacturer to manufacturer in both material and value, and typically have a tolerance of 20%. Inductors have an inherent DC resistance (known as the DCR) that impacts the performance of the output stage. Minimizing the DCR improves the overall performance of the converter. For that application it requires a high load current, it is recommended to select an inductor with a low DCR. The DCR is smaller for lower inductor values, but there is a trade-off between inductance and ripple current; the lower the inductance, the higher the ripple current through the inductor. A minimum inductance must be met in order to meet the ripple current requirements of the specific application circuit.

The output capacitance directly affects the output voltage of the converter and the response time of the output feedback loop, also the amount of output voltage overshoot that occurs during changes in load current. A ripple voltage exists on the DC output as the current through the inductor and capacitor increases and decreases. Increasing the value of output capacitance value reduces the amount of voltage ripple present in the circuit.

However, there is a trade-off between capacitance and the output response. Increasing the capacitance reduces the output voltage ripple and output voltage overshoot, but increases the response time it takes output voltage feedback loop to respond to changes in load. Therefore, a minimum capacitance must be considered, in order to reduce the ripple voltage and voltage overshoot requirements of the converter, while maintaining a feedback loop that can respond quickly enough to load changes. Capacitors also have a parasitic series resistance, known as the equivalent series resistance (ESR). The steady state capacitor value is 0A shown in figure 1.7.

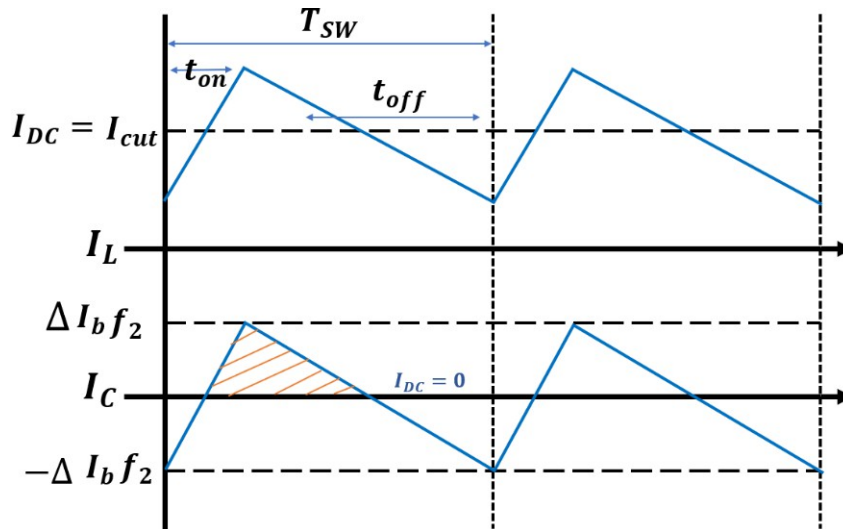


Fig.1.7.ZETA converter's component currents during DCM

G. Summary

The SEPIC converter, the ZETA converter is another converter topology to provide a regulated output voltage from an input voltage that varies above and below the output voltage. The benefits of the ZETA converter over the SEPIC converter include lower output voltage ripple and easier compensation. The drawbacks are the requirements for a higher input voltage ripple, a much larger flying capacitor, and a buck controller (like the TPS40200) capable of driving a high-side PMOS.

The two-stage approach secures a minimum total stress on the circuit components. Further research in PFC systems should be directed towards optimizing the PFC stage and/or the DC/DC stage. It is misunderstood that reducing the number of stages and/or processing less power automatically achieves higher efficiency. Proper design and proper power processing achieve high efficiency. In general, low component stress can be translated into high efficiency, small physical size and low cost. In the low power ranges some of the alternative solutions can have an advantage in cost compared to the two-stage solution but the efficiency will be sacrificed.

This paper discusses the control of the output voltage of a DC step-up converter by varying the input voltage from a single PV source with the help of fuzzy logic. The investigation was conducted through simulation and implementation, with the variation of PV input and load being tested. Research has discovered that the Zeta Converter can increase the output voltage to 24V with a minimum input voltage of 17V while maintaining an average efficiency of 85.83 percent during the simulation and 71.9 percent during implementation. With a variety of input voltages, the fuzzy algorithm can maintain a constant output voltage of 24V. Fuzzy requires an average response time of 3 seconds to increase the voltage and 2 seconds to decrease the voltage on average.

II. SYSTEM OVERVIEW

A. Introduction

The bridgeless isolated Zeta-Luo converter with PF Preregulation is a two-stage converter that consists of a PF Preregulation stage and a bridgeless isolated Zeta-Luo converter stage.

The PF Preregulation stage draws a sinusoidal current from the AC mains and converts it to a high-voltage DC voltage. The bridgeless isolated Zeta–Luo converter stage then converts this high-voltage DC voltage to a low-voltage DC voltage that is suitable for charging the EV battery.

The PF preregulation stage typically consists of a boost converter or a Vienna rectifier. The boost converter is a more common choice, as it is simpler to implement and has a higher efficiency. The Vienna rectifier is a more complex circuit, but it can achieve a higher power factor.

The bridgeless isolated Zeta–Luo converter stage is a combination of the Zeta and Luo converters. It has the advantages of both converters, including a wide input voltage range, high efficiency, and low output voltage ripple.

The bridgeless isolated Zeta–Luo converter-based EV charger with PF preregulation is a complex circuit, but it offers a number of advantages over other conventional EV charger topologies. It has a high efficiency, a wide input voltage range, and a low output voltage ripple. Additionally, the PF preregulation stage ensures that the charger draws a sinusoidal current from the AC mains, even under varying load conditions.

B. Literature Review

A new electric vehicle (EV) charger based on a bridgeless (BL) isolated Zeta–Luo converter with built-in power factor (PF) preregulation capability at the supply side. This configuration is a combination of Zeta and Luo converters, which are designed to work during individual halves of supply voltage. This gives additional benefits of higher efficiency than the previously developed converters on the account of sharing [1].

State of the art and future trends for high power conductive onboard chargers (OBCs) for electric vehicles. To provide a global context, a summary of global charging standards and electric vehicle (EV) related trends are presented, which demonstrates momentum toward the OBCs with higher power rating [2].

Power electronics is an enabling technology for the development of these environmentally friendly vehicle and implementing the advanced electrical architectures to meet the demands for increased electric loads. In this paper, a brief review of the current trends and future vehicle strategies and the function of power electronic subsystems are described [3].

The impact of electric vehicles on power quality in electric distribution system is evaluated. Voltage deviations such as under/over voltage and voltage imbalance are probabilistically quantified using Monte Carlo. Moreover, distribution transformers overload and unbalance are assessed for different vehicle types (i.e., plug-in hybrid and battery electric), different vehicle penetration (up to 50%) while considering level 1 and level 2 charging [4].

The discussion concerning the use of single-stage contrast two-stage PFC solutions has been going on for the last decade and it continues. The purpose of this paper is to direct the focus back on how the power is processed and not so much as to the number of stages or the amount of power processed. The performance of the basic DC/DC topologies is reviewed with focus on the component stress [5].

This converter is designed to operate with adjustable output voltage so that it can operate in two distinct operation modes, depending on the input and output voltages. Therefore, small-signal state-space average models are obtained for the converter operating in step-down and step-up operation modes, and analysis and design of the digital control system are included for different operating points [6].

This paper presents a topology survey evaluating topologies for use in front end ac-dc converters for PHEV battery chargers. The topology survey is focused on several boost power factor corrected converters, which offer high efficiency, high power factor, high density, and low cost. Experimental results are presented and interpreted for five prototype converters, converting universal ac input voltage to 400 V dc [7].

Charger systems are categorized into off-board and on-board types with unidirectional or bidirectional power flow. Unidirectional charging limits hardware requirements and simplifies interconnection issues. Bidirectional charging supports battery energy injection back to the grid. Typical on-board chargers restrict power because of weight, space, and cost constraints. They can be integrated with the electric drive to avoid these problems. The availability of charging infrastructure reduces on-board energy storage requirements and costs. On-board charger systems can be conductive or inductive. An off-board charger can be designed for high charging rates and is less constrained by size and weight. Level 1 (convenience), Level 2 (primary), and Level 3 (fast) power levels are discussed. Future aspects such as roadbed charging are presented. Various power level chargers and infrastructure configurations are presented, compared, and evaluated based on amount of power, charging time and location, cost, equipment, and other factors [8].

In this article, the research of battery chargers in boost charge mode is performed using a mathematical model in EMTP-RV program. During research the root-mean-square value of current ripples were defined while different types of batteries supplying.

The effect of battery chargers' filters, battery internal resistance and permanent load current on current ripples is considered. It is shown, that thyristor battery chargers without filters is fall short of normative current ripples requirements, that can lead to battery service life decrease and filter use doesn't always allow to solve this problem [9].

Solid-state switch mode AC-DC converters having high-frequency transformer isolation are developed in buck, boost, and buck-boost configurations with improved power quality in terms of reduced total harmonic distortion (THD) of input current, power-factor correction (PFC) at AC mains and precisely regulated and isolated DC output voltage feeding to loads from few Watts to several kW. This paper presents a comprehensive study on state of art of power factor corrected single-phase AC-DC converters configurations, control strategies, selection of components and design considerations, performance evaluation, power quality considerations, selection criteria and potential applications, latest trends, and future developments. Simulation results as well as comparative performance are presented and discussed for most of the proposed topologies [11].

A bridgeless buck power factor correction rectifier that substantially improves efficiency at low line of the universal-line range is introduced. By eliminating input bridge diodes, the proposed rectifiers efficiency is further improved. Moreover, the rectifier doubles its output voltage, which extends useable energy of the bulk capacitor after a drop out of the line voltage. The operation and performance of the proposed circuit was verified on a 700-W, universal-line experimental prototype operating at 65 kHz. The measured efficiencies at 50% load from 115 and 230 V line are both close to 96.4%. The efficiency difference between low line and high line is less than 0.5% at full load. A second-stage half-bridge converter was also included to show that the combined power stages easily meet Climate Saver Computing Initiative Gold Standard [12].

This paper proposes a novel single-phase single-stage ac-dc converter with high-frequency isolation and power factor correction. Unlike the two-stage ac-dc converters, the high-frequency pulsating voltage is obtained directly from the power factor correction semi stage and is applied directly to the dc-dc semi stage. The proposed topology is designed to be operated in the continuous conduction mode (CCM), and therefore, there is no need for additional input filter. In addition, the interleaving operation helps reducing the current stress and gets a better electro-magnetic interference performance. Moreover, all of the power switches in the proposed topology can achieve soft-switching commutation. Furthermore, the intermediate dc-link capacitor is no longer directly connected to the dc-dc stage and the capacitance can be reduced greatly; therefore, the bulk capacitor is replaced by a film capacitor. Frequency characteristics and time-domain analysis of the LLC resonant tank is presented in this paper to analyse the characteristics of the proposed converter. Finally, a prototype that converts universal input voltage ranging from 110 to 220 V into 400-V dc output was built and tested to verify the analysis [13].

A new method for deriving isolated buck-boost (IBB) converter with single-stage power conversion is proposed in this paper and novel IBB converters based on high-frequency bridgeless-interleaved boost rectifiers are presented. The semiconductor, conduction losses, and switching losses are reduced significantly by integrating the interleaved boost converters into the full-bridge diode-rectifier. Various high frequency bridgeless boost rectifiers are harvested based on different types of interleaved boost converters, including the conventional boost converter and high step up boost converters with voltage multiplier, and coupled inductor. The full bridge IBB converter with voltage multiplier is analyzed in detail. The voltage multiplier helps to enhance the voltage gain and reduce the voltage stresses of the semiconductors in the rectification circuit [14].

This paper proposes a soft-switched interleaved boost converter with minimal conduction loss increment and removed reverse-recovery problem. The soft-switching operation is enabled by a soft-switching cell composed of passive components in which an auxiliary coupled inductor and a dc-link capacitor are connected between the switch legs of the interleaved boost modules and output stage. Every MOSFET switch of the proposed boost converter operates with zero-voltage switching turn-on using the coupled inductor current. Consequently, the switching loss of the proposed interleaved boost converter is greatly reduced. In addition, the reduced circulating current in the auxiliary circuit minimizes the increment of the conduction loss. The proposed soft-switched interleaved boost converter operation is verified with 500-W experimental results [15].

As a key component of a plug-in hybrid electric vehicle (PHEV) charger system, the front-end ac-dc converter must achieve high efficiency and power density. This paper presents a topology survey evaluating topologies for use in front-end ac-dc converters for PHEV battery chargers. The topology survey is focused on several boost power factor corrected converters, which offer high efficiency, high power factor, high density, and low cost. Experimental results are presented and interpreted for five prototype converters, converting universal ac input voltage to 400 V dc [16].

This paper presents the dynamic modeling and digital control of a single-stage isolated current rectifier with power factor correction based on the integration of full-bridge and flyback converters. This converter is designed to operate with adjustable output voltage so that it can operate in two distinct operation modes, depending on the input and output voltages.

Therefore, small-signal state-space average models are obtained for the converter operating in step-down and step-up operation modes, and analysis and design of the digital control system are included for different operating points. Experimental results based on a 3-kW prototype are presented to validate the proposed control system under distinct conditions [17].

C. Summary

The literature review on the design and control circuit for Zeta Luo converters in electric vehicle battery chargers reveals a significant focus on enhancing efficiency, reducing size, and improving control strategies. Studies emphasize the importance of optimal design parameters, such as component selection, topology modifications, and control techniques, to achieve high efficiency, fast charging, and compatibility with varying battery technologies. Challenges, including high-frequency switching, electromagnetic interference, and thermal management, have been addressed through innovative circuit topologies and control algorithms. Despite advancements, further research is needed to optimize performance, increase power density, and ensure robustness in real-world applications for efficient and reliable electric vehicle charging systems. This brief introduces an isolated two-switch Zeta dc-dc converter, along with the steady-state analysis and experimentation.

The high transistor voltage stress due to the ringing caused by the resonance of the transformer leakage inductance and the transistor output capacitance is a major drawback in the conventional isolated Zeta converter. With the incorporation of an additional transistor and two clamping diodes on the primary side of the transformer of the isolated Zeta converter, an isolated two transistor Zeta converter is proposed. In the proposed converter, the voltage stress of both transistors is reduced to the dc input voltage. Experimental results from a 10-V/30-W 100-kHz laboratory prototype are presented to validate the theoretical analysis. The two transistors plus the clamping diodes on the primary side of the transformer provide a simple mechanism to limit the switch overvoltage, which occurs in the isolated single-transistor Zeta converter. The theoretical analysis has been verified by experimental results. The clamping of the switch over voltages has been achieved. The power transistors have been turned on under reduced voltage stresses. The analysis and experimental results provide a basic understanding of the converter behaviour. The proposed isolated two-switch Zeta converter is a simple topology and can be of high practical value for various industrial applications such as universal input adapters/charges for cell phones, laptop, and computers; and power supplies for telecommunication equipment, digital video disc players, and light emitting diode displays. Future work constitutes the modelling

III. SYSTEM DESCRIPTION

A. Introduction

To ensure reduced electromagnetic interference at input and to obtain low switching device losses, a single-stage resonant converter is discussed for EV. However, the need for four switches to integrate the operation of boost and full bridge LLC converter results into a complex design process of the PFC converter, which is not recommended at sudden varying voltages. Another boost-fed full-bridge converter for EV chargers, which has the obvious demerits with increased components and circuit complexity, as well as a complex control algorithm need to be developed for four gate drivers. Therefore, to retain the benefits of improved power density and high efficiency, as well as to provide simple control, various off-board solutions for unidirectional EV chargers.

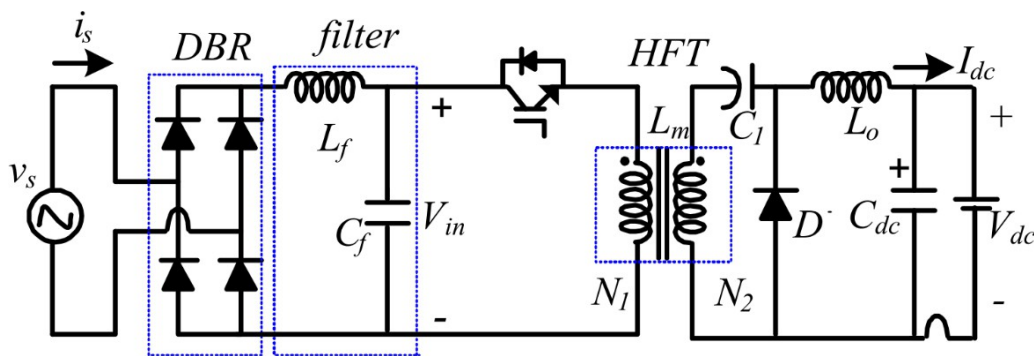


Fig.3.1. Circuit configuration of Isolated Zeta converter

However, a single-stage isolated PFC converter with input DBR comes out to be lossy, which results into poor charging efficiency due to the increased conduction loss.

Theunidirectional battery chargers incorporate the popular boost PF preregulator for the intrinsic PFC operation. However, at high power, conventional buck and boost converters are found unsuitable, as the current wave-shaping characteristic is not effective, at zero crossing in the buck converter. Moreover, the boost converter shows restricted change in duty cycle over the fluctuation in line voltage. This restriction in the duty cycle is avoided using buck–boost converters, for PF preregulationatthecharger mains, asthedutycycle may vary effectively over the completerange of line voltages. A detail review and design guidelines for buck–boost-based high-frequency isolatedimprovedPQconverters(IPQCs)arepresentedintheliterature.Thedifferentbuck–boost based configurations such as flyback, single-ended primary inductor converter (SEPIC), Cuk, Luo and Zeta converters for PF preregulation in several single-phase applications.

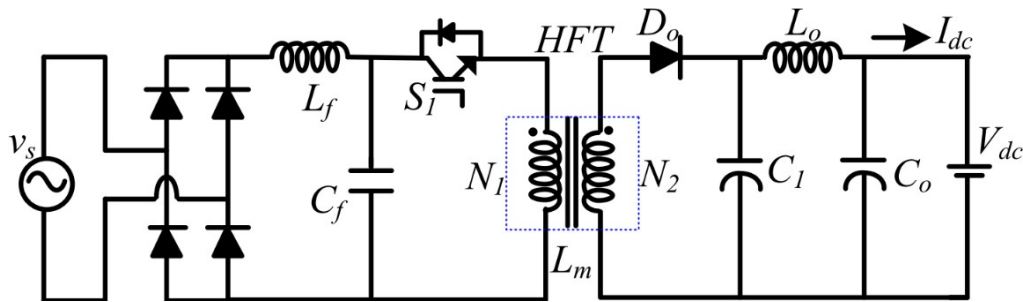


Fig.3.2.CircuitconfigurationofIsolatedLuoconverter

The disadvantage of pulsating output current and the large size of filters to minimize the output charge ripple in the single-stage isolated SEPIC converter makes it unsuitable for the PF preregulated charger. The Cuk converter is quite popular in this range as reduced ripple at both the input and output end is achieved. However, it requires series capacitor with high rms current for operation at increased rating. The Zeta and Luo converters both offer excellent PQ improvement features, good light load regulation, and the advantage of low ripple in charging current, as well, when used in combination.

The configuration of this BL isolated Zeta–Luo converter-based vehicle charger is obtained by the integration of BL isolated Zeta and Luo converters, which conduct in two separate halfcycles, independently. The operation of the BL converter is achieved in the discontinuous mode of operation to provide PF pre-regulation at the rated and over wider range of varying mains voltages. During the operation of the Zeta converter, the semiconductor switch S_1 , transformer magnetizing inductance L_{m1} , intermediate capacitor C_1 , and output diode D_{o1} conduct during positive half of the supply cycle. However, the operation of the Luo converter during the negative half of the supply is assisted with the semiconductor switch S_2 , transformer magnetizing inductance L_{m2} , intermediate capacitor C_2 , and output diode D_{o2} . The theoretical analysis during the steady-state operation of this BL isolated converter is detailed as follows

To improve the charger efficiency, many bridgeless (BL) PFC converter topologies with isolation are reported in the literature. This reduces the semiconductor losses as several diodes, which conduct over a switching cycle, are reduced to half. The circuit configuration of conventional isolated Zeta and Luo converters is shown in Fig. 3.1 and 3.2. Therefore, based on above mentioned DBR-based topologies, an EV charger with an integrated BL isolated Zeta–Luo configuration, as shown in Fig. 3.3, is developed as per the design expressions, in this work. The charging of a 48 V, 100 Ah EV battery is identified in the constant current and constant voltage (CC–CV) modes using a cascaded proportional-integral (PI) controller.

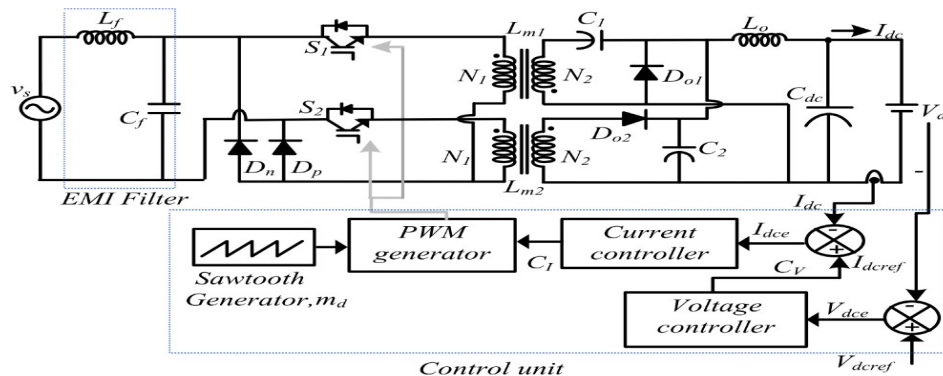


Fig.3.3CircuitconfigurationofBLisolatedZeta–Luoconverter-basedcharger.

This new BL converter is designed to operate independently during the respective positive and negative supply cycles in either the Zeta or Luo mode. This gives the additional benefits of high efficiency than the previously developed converters on the account of sharing the output inductors for both converters. The topology offers the advantage of reduced number of components as compared to other BL configurations due to the integration of two different converters. The significant features and contribution of this charger configuration are listed as follows.

- 1) The number of output inductors are reduced due to integration of Zeta–Luo converters in two half cycles. This gives significant reduction in the size of the charger.
- 2) Over a switching cycle, the current conduction is seen to be a reduced number of components and devices; which, comparatively, gives the improvement in efficiency.
- 3) The value of the magnetizing inductance of this isolated converter is selected such as the converter remains in the discontinuous conduction mode (DCM), which is beneficial for the charger with the reduced size and low cost.
- 4) The control of the PFC converter is easy to implement as similar pulses are given to both switches in each line cycle. The robust performance of this new BL isolated EV charger is found satisfactory during the charging operation at the steady state as well as over the change in line voltage and loads. The performance indices at utility such as mains PF, DPF, supply current THD, are seen to comply with the recommended PQ regulations.

B. Operation of BL Isolated Converter

Three different operating modes and associated key operation of this isolated converter, in Zeta and Luo modes for the corresponding supply halves, are illustrated as follows.

Mode-I [t_0-t_1]: During this mode, gate pulse to switch S1 is given at instant to. The magnetizing current in the inductance L_{m1} builds up linearly, as it stores the energy from the source via the line diode D_p . The voltage across the energy transfer capacitor C_1 starts decreasing as current finds a path through the output inductor L_{o1} at the secondary side, as shown in Fig.3.1. The output diode D_{o1} is seen to be in the nonconducting state during this interval. This mode ends at t_1 , when switch S1 is turned OFF.

Fig.3.4. Operation of Zeta–Luo converter for three switching states Mode-I Zeta mode

Mode-II [t_1-t_2]: During this interval, switch S1, is turned OFF and diode D_{o1} starts conducting. The magnetizing inductance L_{m1} releases the stored energy via capacitor C_1 to output diode D_{o1} and at secondary winding of the transformer. The output dc-link capacitor starts charging through the inductance L_o and the battery current is obtained in the CC mode.

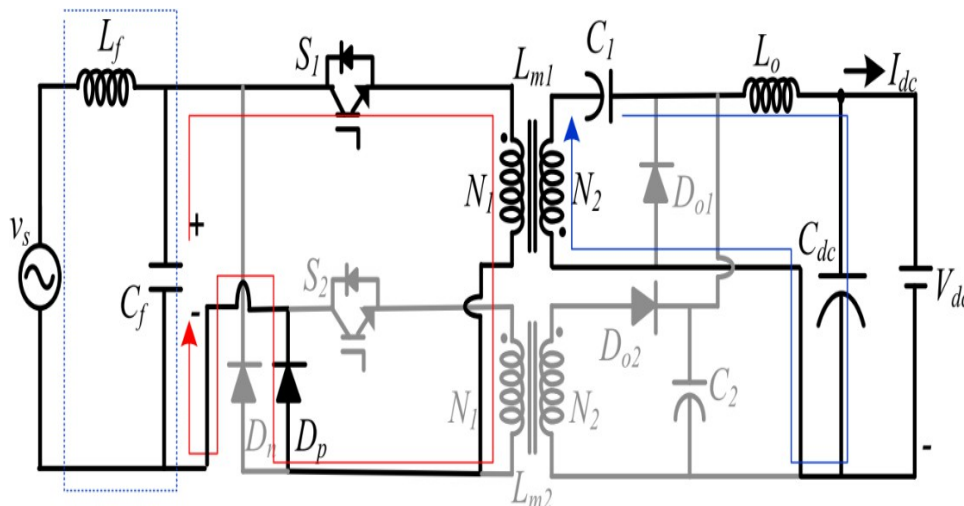


Fig.3.5. Operation of Zeta–Luo converter for three switching states Mode-II Zeta mode

Mode-III [t_1-t_3]: During this interval, switch S1 remains OFF and the converter enters the DCM mode. The sum of currents through the magnetizing inductor L_{m1} and output inductance L_{o1} leads to the zero current through the diode D_{o1} , as shown in Figs. 3.3 and Fig.3.4. The capacitor C_{dc} continues to supply charging current to the battery.

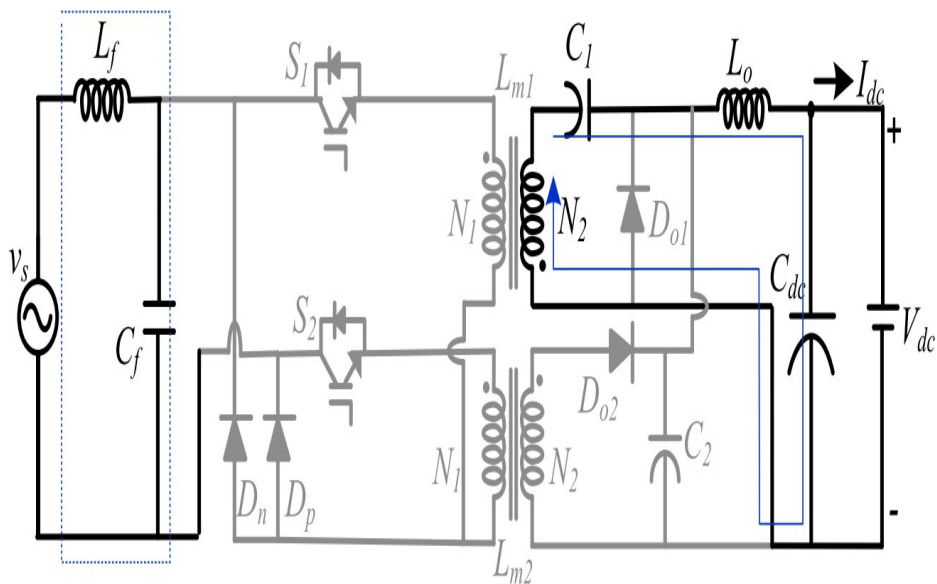


Fig.3.6 Operation of Zeta-Luo converter for three switching states Mode-III Zeta mode

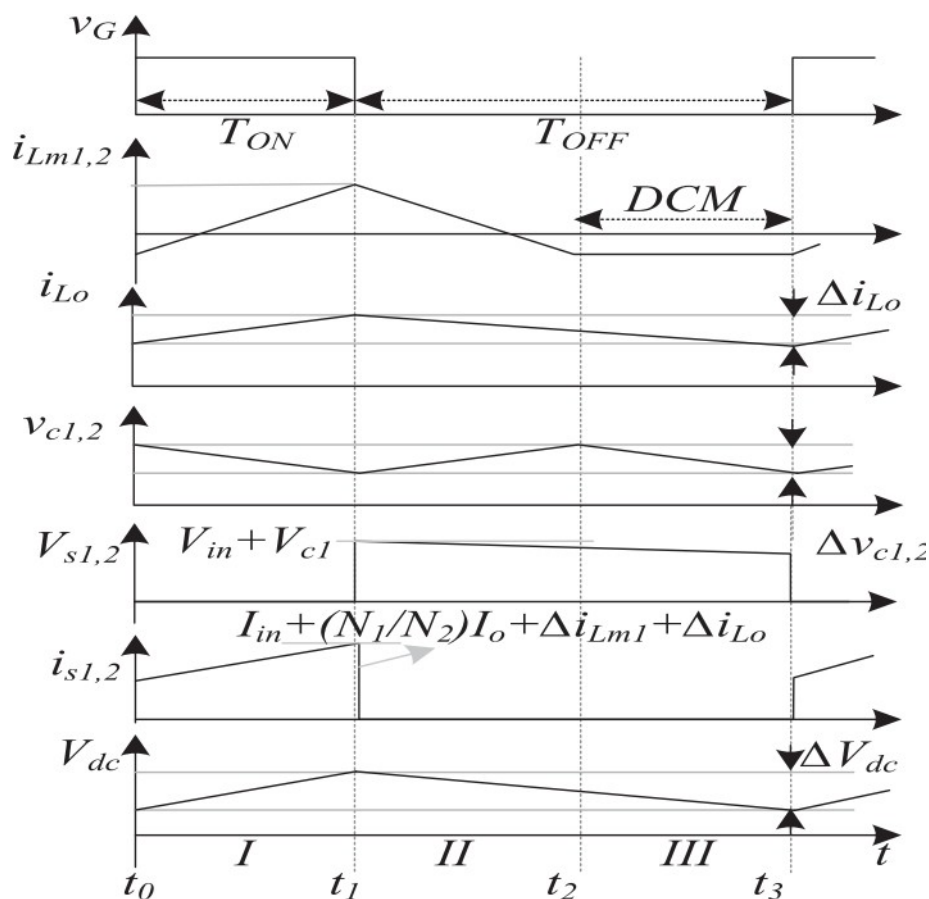


Fig.3.7. Charging and discharging sequence of different components over a switching cycle for Zeta and Luo modes.

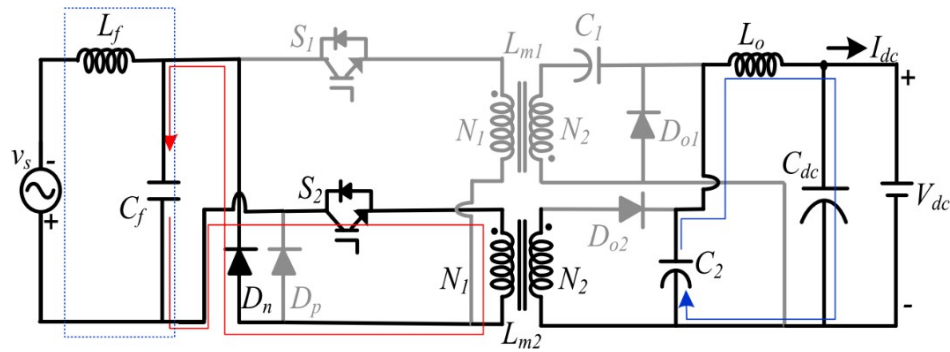


Fig.3.8 Operation of Zeta-Luo converter for three switching states Mode-I Luo mode

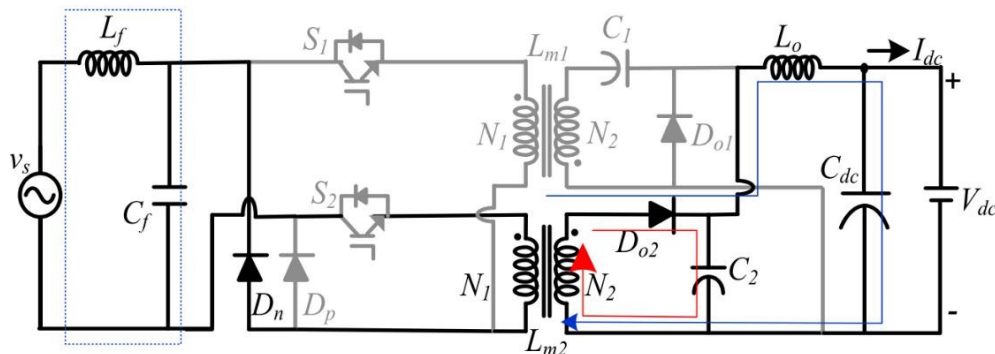


Fig.3.9 Operation of Zeta-Luo converter for three switching states Mode-II Luo mode (-ve half line).

The similar sequences of operations are observed in the Luo mode during the negative half, as shown in Fig. 3.9. The only difference is that the DCM operation in the Luo converter is identified with the zero current in the magnetizing inductance. Fig. 3.4 shows the associated waveforms of different switching components over a switching cycle.

C. Summary

The Zeta-Luo converter is a bridgeless isolated dc-dc converter that operates in three different modes: Zeta mode during the positive half of the input voltage cycle and Luo mode during the negative half of the input voltage cycle. The third mode is the DCM mode, which occurs when the current through the magnetizing inductor or output inductor reaches zero. The Zeta-Luo converter is a promising topology for a wide range of applications, including electric vehicle chargers, battery-powered systems, and renewable energy systems.

IV. SYSTEM DESIGN

A. Introduction

The design of a Zeta-Luo converter system typically involves the following steps:

- 1) **Topology selection:** The first step is to select the appropriate Zeta-Luo converter topology for the desired application. There are several different Zeta-Luo converter topologies available, each with its own advantages and disadvantages. The most common topology is the single-stage Zeta-Luo converter, which is relatively simple to implement and control. However, there are also dual-stage and multi-stage Zeta-Luo converter topologies that can offer improved performance for specific applications.
- 2) **Component selection:** Once the topology has been selected, the next step is to select the appropriate components for the converter. The components must be selected carefully to ensure that they can handle the required power and voltage levels. The most important components to select are the power switches, transformer, and inductors.

B. Battery Control

The two semiconductor switches of the BL isolated converter operate independently but in synchronism during one switching cycle. Both the pulses to the converter devices are generated in a similar pattern using a cascaded PI controller.

The controller uses a current controller to maintain a CC through the battery up to 80% state of charge (SOC) and a voltage controller, which controls the reduced battery current up to full SOC. For CC charging, after sensing the battery current I_{dc} , it is compared to the reference current $I_{dc_{ref}}$, which is controlled using the voltage PI controller. This comparison leads to an error signal I_{dc_e} , which is obtained at given sampling instant k , using the expression as

$$I_{dc_e}(K) = I_{dc_{ref}}(K) - I_{dc}(K) \tag{1}$$

This error I_{dc_e} , after a comparison, is given to a current PI controller, which gives a control signal C_i at the controller output. At a given instant k , signal C_i is expressed as

$$C_i(K) = C_i(K-1) + K_{pi} \{ I_{dc_e}(K) - I_{dc_e}(K-1) \} + K_{il} I_{dc_e}(K) \tag{2}$$

Where K_{pi} and K_{il} are the proportional (P) and integral (I) gain constants for tuned current PI controller. The input to the voltage PI controller is the error V_{dc_e} , which is the result of comparison of two quantities, i.e., sensed voltage V_{dc} and the reference voltage $V_{dc_{ref}}$. The reference limit is set at the battery voltage corresponding to 100% SOC. The output of the voltage controller is the signal C_v , which is used for current reference in the CC mode. The error signal and control voltage C_v for a given sampling instant k are expressed as

$$\begin{aligned} V_{dc_e}(K) &= V_{dc_{ref}}(K) - V_{dc}(K) \\ C_v(K) &= C_v(K-1) + K_{pv} \{ V_{dc_e}(K) - V_{dc_e}(K-1) \} + K_{iv} V_{dc_e}(K) \end{aligned} \tag{3}$$

Where K_{pv} is the proportional and K_{iv} is the integral gain constant for voltage control. The required gating sequence for two semiconductor devices is obtained after comparing the control signal C_i to a high-frequency carrier (m_d). The converter duty cycle is varied over a wide range to ensure an intrinsic PF preregulation over all the operating conditions.

C. Design Of EV Charger

This BL isolated converter is designed in DCM for 780 W (P) rating, and magnetizing inductance of a high-frequency transformer (HFT) is selected such as operation of the output diode Do_1 or Do_2 ceases at the end of each switching period. The supply voltage at the input of this isolated converter, is expressed as

$$v_s(t) = V_{sm} \sin(2\pi ft) = 311 \sin(2\pi \cdot 50t) \tag{4}$$

where V_s and f are rms source voltage (peak value $V_{spk} = V_s \sqrt{2}$) and frequency (Hz) of line voltage, respectively. The expression to calculate the voltage (V_{dc}) is given as

$$V_{dc} = \frac{N_2}{N_1} \frac{D V_{in}}{1-D} \tag{5}$$

where D is the duty ratio of this isolated converter in Zeta or Luomodes and n is the turns ratio of the transformer. This value is considered as 0.5, which results into the calculated value of the instantaneous duty cycle (D) as

$$D(t) = \frac{V_{dc}}{\left(\frac{N_2}{N_1}\right) V_{in}(t) + V_{dc}} \tag{6}$$

To achieve a built-in PF preregulation over the supply voltage variation range of 160–260 V, the duty ratio (D_a and D_b) is estimated as 0.35 and 0.26, respectively, for charging duration. To obtain the DCM operation, the magnetizing inductance $L_{m1,2}$ is selected for an allowable current ripple of two times the input current. The calculation for the critical magnetizing

$$\begin{aligned} I_{m1,2c} &= \left(\frac{V_{smin}^2}{P} \right) \frac{T_s V_{dc}}{2n v_{in} + V_{dc}} \\ &= \left(\frac{160^2}{780} \right) \frac{1}{2 \times 20000} \frac{V_{dc} \cdot 0.5 \times 1}{60\sqrt{2} + 65} \\ &= 0.295 \text{ mH} \end{aligned} \tag{7}$$

here $T_s (= 1/f_s)$ is the switching period for this isolated converter, selected as $50 \mu s$ ($1/20 \text{ kHz}$). The magnetizing inductance ($L_{m1,2c}$) is selected lower than the calculated one, i.e., 0.1 mH or $100 \mu H$ to prevent the current through the diode at the end of every switching interval. For a voltage ripple (γ) of 20% in the voltage across the intermediate capacitances $C_{1,2}$ and to transfer the energy efficiently from HFT primary to secondary winding, the value of intermediate capacitor $C_{1,2}$ is obtained as

$$\begin{aligned}
 C_{1,2} &= \frac{v_{in} n^2 \{D(t)\}^2}{\Delta V_{w1,2}(t) R_d \omega f_s \{1-D(t)\}} \tag{8} \\
 &= \frac{nP}{\gamma \sqrt{2} V_{smax} f_s (n \sqrt{2} V_{smax} + V_{dc})} \\
 &= \frac{0.5 \times 780}{0.2 \times 260 \sqrt{2} \times 20000 \times (0.5 \times 260 \sqrt{2} + 65)}
 \end{aligned}$$

The value of intermediate capacitances is obtained as $1.03 \mu F$, which is calculated at rated dc voltage and maximum source voltage (i.e., $V_{smax} = 260 \text{ V}$). Therefore, to ensure the continuity in energy transfer, over a switching interval, a $1 \mu F$ value is selected in this application. To ensure the continuity in the output current and for an allowable ripple current of 20% at the output, the estimation for output inductance L_o , is given as

$$\begin{aligned}
 I_o &= \left(\frac{V_{smin}^2}{P} \right) \frac{V_{dc}}{k \sqrt{2} V_{smin} f_s} \frac{V_{dc}}{n v_{in} + V_{dc}} \tag{9} \\
 &= \left(\frac{160^2}{780} \right) \frac{65}{0.2 \sqrt{2} \times 160 \times 20000} \frac{65}{0.5 \times 160 \sqrt{2} + 65} \\
 &= 0.795 \text{ mH}
 \end{aligned}$$

Therefore, a value of L_o is chosen as 0.8 mH here. To avoid the second harmonic ripple in charging current, the estimation of capacitor C_{dc} , for an allowable ripple voltage of 3%, is achieved as

$$\begin{aligned}
 C_{dc} &= \frac{I_{dc}}{2\omega \Delta V_{dc}} = \frac{(P/V_{dc})}{2\omega \Delta V_{dc}} = \frac{P}{2\omega \Delta V_{dc}^2} \tag{10} \\
 &= \frac{780}{2 \times 314 \times 0.03 \times 65^2}
 \end{aligned}$$

where ω is the supply frequency (rad/s) and Δ depicts the ripple in converter dc-link voltage. Therefore, a 10 mF value is selected for dc-link capacitance. To avoid the travelling of switching harmonics toward the ac source, an LC-based low-pass filter is designed using the following expressions:

$$\begin{aligned}
 C_f \leq C_{fmax} \quad , C_{fmax} &= \frac{\frac{rVZ}{V_s}}{(\omega \sqrt{2} V_s)} \tan(\cos^{-1} DPF) \tag{11} \\
 &= \frac{180 \sqrt{47440}}{(314 \times 311)} \tan 1^\circ = 896 \text{ nF}
 \end{aligned}$$

where θ is expressed as the angle by which the line current leads or lags the line voltage, assumed to be 1° , DPF is the displacement power factor. The estimated value of C_{fmax} is achieved as 580 nF for this work. Now considering the filter cut frequency as $f_{cr} < f_s/10$, the inductance L , is calculated as

$$L_f = \frac{1}{4 \times \pi^2 \times f_{cr}^2 \times C_f}$$

$$= \frac{1}{4 \times \pi^2 \times 5000^2 \times 580 \times 10^{-9}}$$

$$= 1.7 \text{ mH}$$

D. Summary

The design of a bridgeless isolated Zeta-Luo converter-based EV charger with PF pre-regulation. The authors compare this topology to other existing EV charger topologies and discuss its advantages, such as reduced component count, improved efficiency, and simpler control. The authors also discuss the design considerations for the proposed converter, such as the selection of the magnetizing inductance to ensure that the converter operates in discontinuous conduction mode.

V. SIMULATION RESULTS

A. Introduction

Performance of a BL isolated converter-based charger for high power quality is verified. Simulation results are recorded for CC-CV charging, and the explanation for the performance at the steady state and for change in load current and line voltage is given as follows.

B. Validation & Results

Performance of a BL isolated converter-based charger for high power quality is verified on a laboratory prototype with a 48 V 100 Ah battery-based interface is used for control and power circuits of this charger. The picture of developed setup is shown in Fig. 5.1. Test results are recorded for CC-CV charging, and the explanation for the performance at the steady state and for change in load current and line voltage is given as follows.

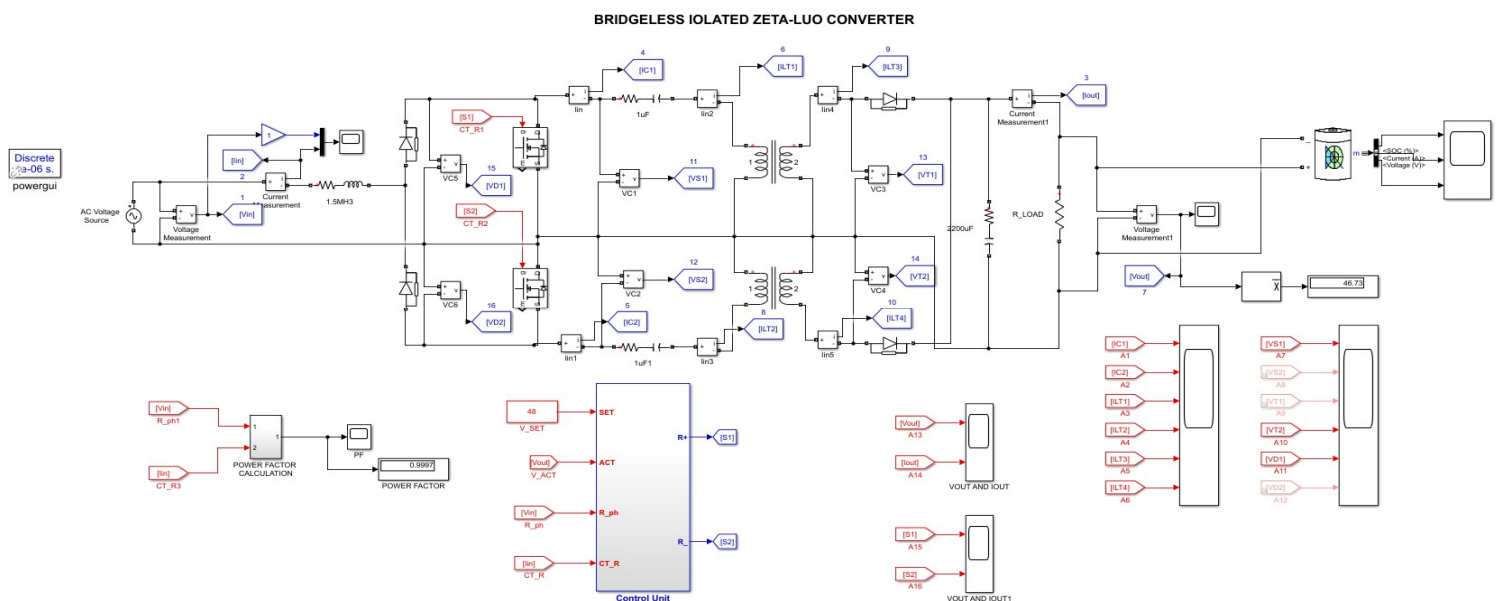


Fig.,5.1,Circuit Diagram for Zeta-Luo Converter

1) PFP Preregulation of Charger

The steady-state high PQ operation of this charger is shown as per Fig. 5.1, which records the waveforms of the battery voltage V_{dc} and the battery current I_{dc} with the line voltage v_s and line current i_s . It is clear from the battery current waveform that for this new charger, the integration of the Zeta and Luo converter reduces the ripple in charging current as the output inductor is shared in both modes. Therefore, a smooth charging current is available for the battery.

The ripple in battery current is seen as the ripples affect the battery health in long-term applications.

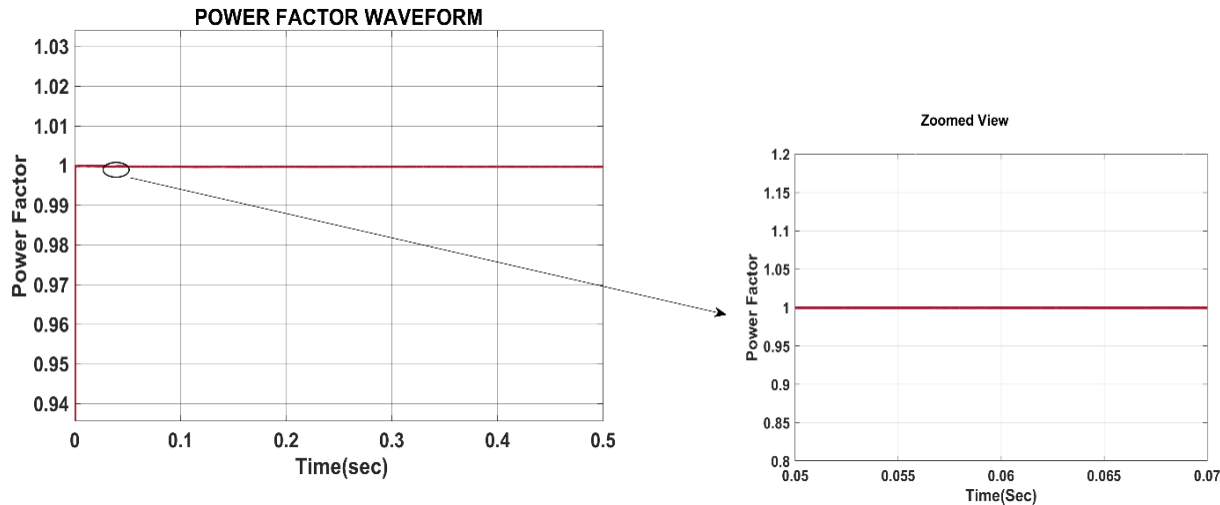


Fig.5.2, Power Factor Waveform

2) Converter Performance

at Steady State The performance of the charger with the BL isolated converter is validated at the steady state, as per Fig. 5.2. This converter works in BL configuration with Zeta operation in positive half line and with Luo operation in negative half line. As shown in Fig. 5.3 the performance of primary side energy transfer capacitors is found satisfactory with the continuous voltage seen across them over a switching cycle. The capacitors C_1, C_2 work in Zeta and Luo modes during the positive and negative half cycles, respectively. Similarly, the waveforms of the output inductor currents in CCM are recorded for two modes, showing the measured voltage across and current through the PFP switches S_1, S_2 , which clearly demonstrates an acceptable range of peak voltage stress at 510 V and current stress limit of 35 A for 780 W design. It is obvious that the incorporation of the Luo converter in the negative half cycle avoids the use of an extra inductor due to sharing of output stage of charger. Moreover, the use of output inductance at both halves also minimizes the pulsation in output current, then that in case the Zeta converter used for both cycles. It is implied from Figure that this charger operates in DCM. The selected value of magnetizing inductances of the HF transformer $L_{m1,2}$ are an appropriate range to ensure discontinuous current through both the windings, during a switching cycle, as well as over the respective half cycle.

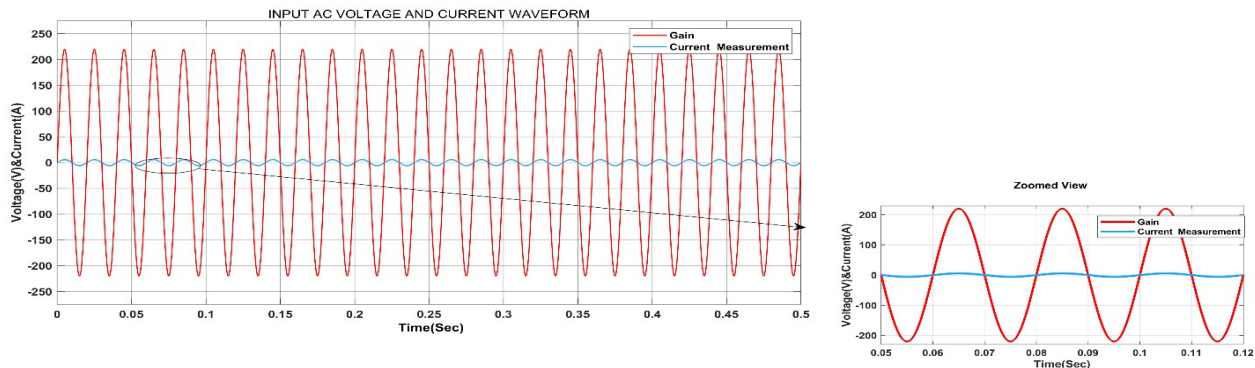


Fig.5.3, Input AC Voltage and Current waveform

3) UPF Operation at Different Line Voltages

The operation of this BL isolated converter for high PQ performance is investigated under sudden fluctuations in input voltage. It is to be mentioned that as per Fig.5.2, an improved PF- based charging is validated and the line current THD is lowered to the permissible harmonic's standard during the two-line voltages.

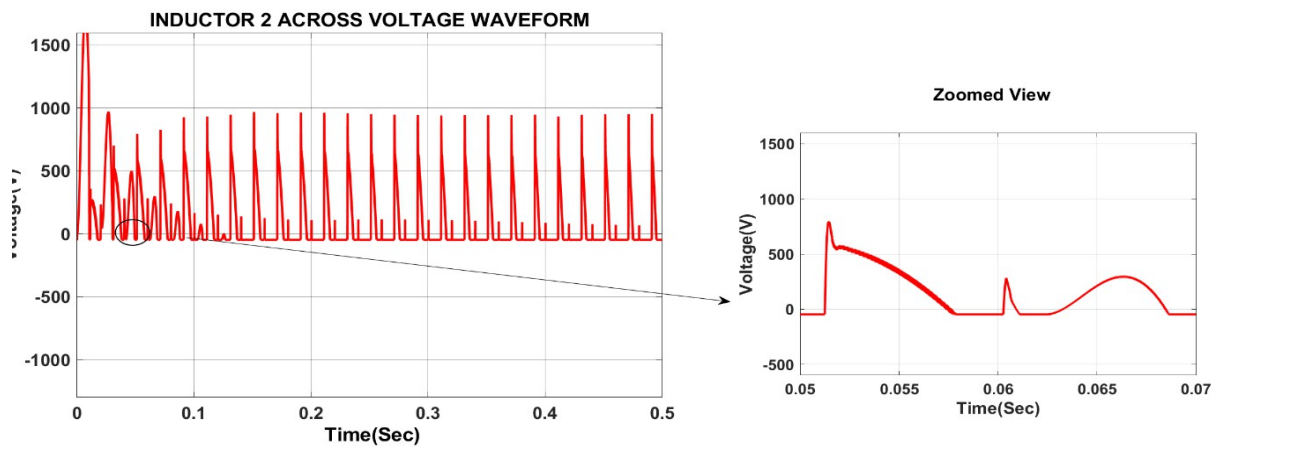


Fig.,5.4, Inductor Voltage Waveform

ACV, V_{dc} is observed across the battery for the complete range of fluctuation. The battery charging during CC charging is observed with constant low ripple, like the rated line condition.

However, to sustain this change in ac voltage from 220 V, an increased and decreased in line current, respectively, for a dip and a hike in line voltage, are recorded, which validate the constant charger output. The improvement in input side indices, such as displacement PF, line PF, crest factor, and THD in line current, are observed as per Figs 5.4. The recorded power profile for the power transfer is shown with apparent power, active power, and reactive power

4) Performance at Variation in Load current

The performance of this charger is validated for step change in load current, i.e., the battery current i_{dc} is changed from 50%. The recorded waveforms of the grid voltage, the grid current, the battery voltage, and the battery current are shown in Fig. 5.6 and Fig. 5.7. To validate the converter performance during increase in the load, a change in the battery current is introduced from 5 to 10 A. A corresponding rise in the grid current is observed as per Figure as the load demand is increased. Similarly, for step reduction in the load demand, the battery current is lowered from rated to 5 A. As a result, a dip in the grid current is recorded. Therefore, despite a step change in the load current, the closed-loop performance of the converter is found satisfactory as shown in Fig.5.5.

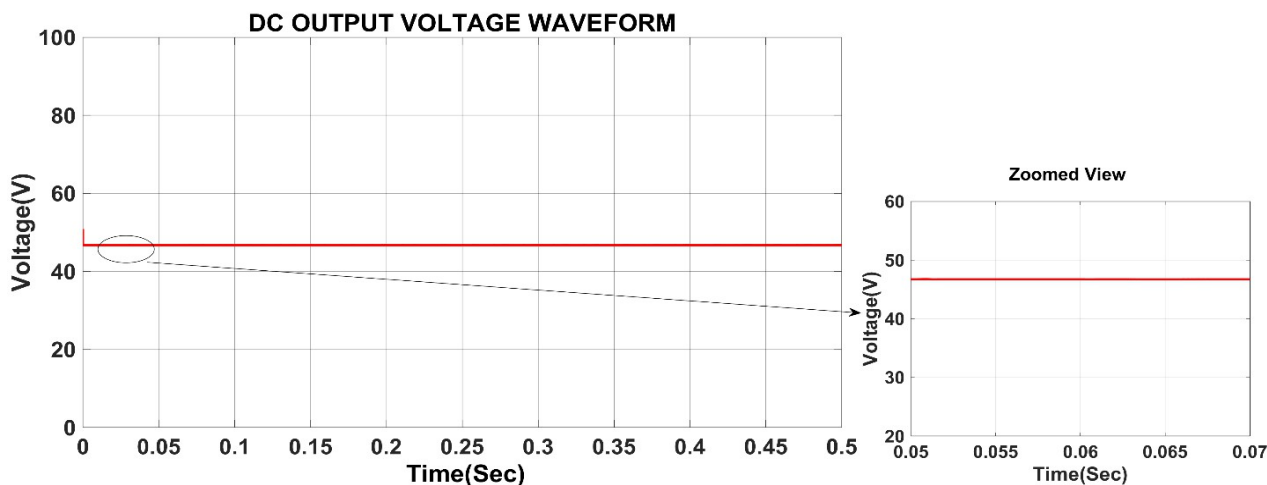


Figure 5.5, DC Output Voltage Waveform

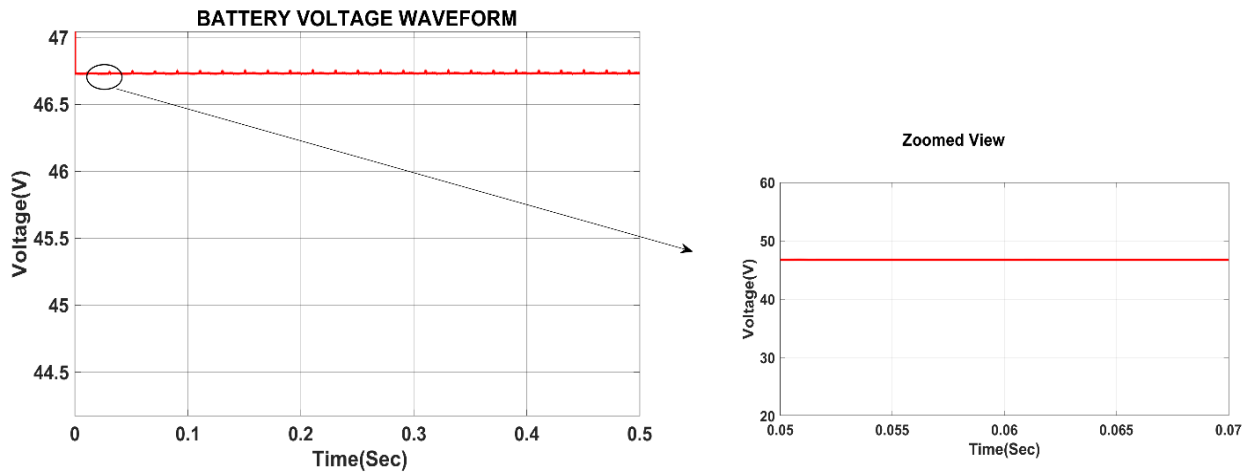


Figure 5.6, Battery Voltage Waveform

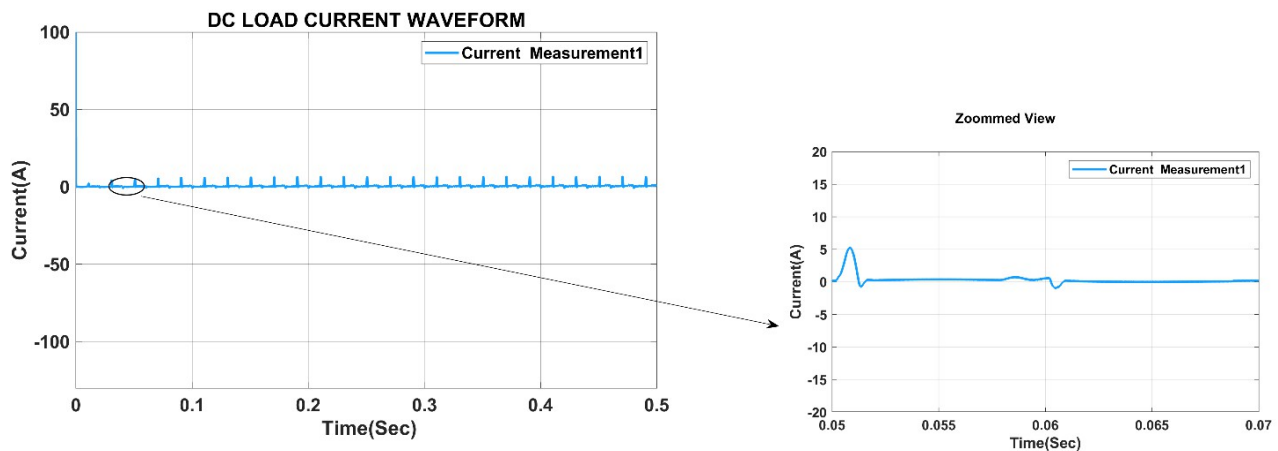


Figure 5.7, DC Load Current Waveforms Waveform

C. Summary

The proposed bridgeless isolated Zeta Luo converter based EV charger is a new type of EV charger that has a higher efficiency than previously developed EV chargers, on account of sharing the output inductors for both converters. It provides a uniform charging current for the battery, due to the presence of output inductance in both converters. Achieves unity power factor (UPF) at steady state and for a variation in mains voltage and loads. The power quality (PQ) indices at the supply side conform to the recommended IEC 61000-3-2 guidelines for all the operating conditions. The experimental verification shows that the proposed EV charger is a promising candidate for future EV charging applications.

VI. CONCLUSION AND NEXT PLANNING

A. Conclusion

The work carried out in the report can be summarized briefly as follows. An improved PQ based BL isolated Zeta Luo converter had been designed in DCM for the EV battery charger. This configuration was achieved with combined Zeta and Luo converters, which were redesigned to work during individual halves of supply voltage. This gives an additional benefit of higher efficiency than the previously developed converters on account of sharing output inductors for both converters.

Therefore, the charger cost and size were reduced. Moreover, a uniform charging current was obtained for the battery due to the presence of an output inductance in both converters, as compared to the Zeta or Luo converter was used for both cycles. Similar pulses were applied to both devices during UPF operation; therefore, the gate drive and control implementation were easy.

The performance of this charger was recorded as per an IEC 61000-3-2 standard guidelines, over the entire operating range of line and loadings. The line current was reshaped to sinusoidal and unity PF was achieved for a complete range of mains voltage. The source current distortion was measured as low as 4.1%, 3.4%, and 4.3% during CC charging and 7.1% during the CV mode. Therefore, this PF preregulation-based BL isolated converter seemed to be an improved solution for commercially cost effective off-board charging. The BL topology and shared output inductors significantly reduce semiconductor losses, leading to improved efficiency. The built-in PF preregulation capability ensures near-unity power factor operation, minimizing reactive power consumption and improving grid stability. The elimination of bridge rectifiers and the sharing of output inductors result in a compact and lightweight charger design. Enhanced performance under sudden voltage variations: The proposed charger exhibits robust performance under sudden line voltage fluctuations, ensuring reliable EV charging even during unstable grid conditions. The Bridgeless Isolated Zeta–Luo Converter-Based EV Charger With PF Preregulation presents a promising solution for efficient and reliable EV charging. Its combination of high efficiency, improved power factor, reduced size, and enhanced performance under voltage variations makes it an attractive choice for future EV charging infrastructure.

B. Next Planning

The planning for the remaining work is given below.

Sr. No.	Details of work completion	Dates	Expected outcomes
1	Closed Loop Simulation	Dec-2023	Closed Loop MATLAB Simulation for Zeta–Luo Converter
2	Hardware	Jan-2024	Purchase of Instruments for model with proper parameters
3	Implementation on hardware	Feb-2024	Connecting the instruments and form Hardware model
4	Report	Feb-2024	Final Project Report

Table.6.1 Next Planning of project

REFERENCES

- [1] C. Mi, M. A. Masrur, and D. W. Gao, *Hybrid Electric Vehicles: Principles and Applications with Practical Perspectives*. Hoboken, NJ, USA: Wiley, 2011.
- [2] V. Krithika and C. Subramani, "A comprehensive review on choice of hybrid vehicles and power converters, control strategies for hybrid electric vehicles," *Int. J. Energy Res.*, vol. 42, no. 5, pp. 1–24, 2018.
- [3] A. Khaligh and M. D'Antonio, "Global trends in high-power on-board chargers for electric vehicles," *IEEE Trans. Veh. Technol.*, vol. 68, no. 4, pp. 3306–3324, Apr. 2019.
- [4] A. Emadi, Y. J. Lee, and K. Rajashekara, "Power electronics and motor drives in electric, hybrid electric, and plug-in hybrid electric vehicles," *IEEE Trans. Ind. Appl.*, vol. 55, no. 6, pp. 2237–2245, Jun. 2008.
- [5] M. Yilmaz and P. T. Krein, "Review of battery charger topologies, charging power levels, and infrastructure for plug-in electric and hybrid vehicles," *IEEE Trans. Power Electron.*, vol. 28, no. 5, pp. 2151–2169, May 2013.
- [6] M. Gray and W. Morsi, "Power quality assessment in distribution systems embedded with plug-in hybrid and battery electric vehicles," *IEEE Trans. Power Syst.*, vol. 30, no. 2, pp. 663–671, Mar. 2015.
- [7] Limits for Harmonics Current Emissions (Equipment Current per Phase), International standards IEC 61000-3-2, 2000.
- [8] L. Petersen and M. Andersen, "Two-stage power factor corrected power supplies: The low component-stress approach," in *Proc. IEEE APEC*, 2002, vol. 2, pp. 1195–1201.
- [9] J. Duarte, L. R. Lima, L. Oliveira, M. Mezaroba, L. Michels, and C. Rech. "Modeling and digital control of a single-stage step-up/down isolated PFC rectifier," *IEEE Trans. Ind. Informat.*, vol. 9, no. 2, pp. 1017–1028, May 2013.
- [10] F. Musavi, M. Edington, W. Eberle, and W. G. Dunford, "Evaluation and efficiency comparison of front-end AC-DC plug-in hybrid charger topologies," *IEEE Trans. Smart Grid*, vol. 3, no. 1, pp. 413–421, Mar. 2012.
- [11] J. Yi, W. Choi, and B. Cho, "Zero-voltage-transition interleaved boost converter with an auxiliary coupled inductor," *IEEE Trans. Power Electron.*, vol. 32, no. 8, pp. 5917–5930, Aug. 2017.



- [12] H.Wu,T.Mu,H.Ge,andY.Xing,"Full-rangesoft-switching-isolatedbuck-boostconverters with integrated interleaved boost converter and phase-shifted control," IEEE Trans. Power Electron., vol. 31, no. 2, pp. 987–999, Feb. 2016.
- [13] G. Li, J. Xia, K. Wang, Y. Deng, X. He, and Y. Wang, "A single-stage interleaved resonant bridgeless boost rectifier with high-frequency isolation," IEEE J. Emerg. Sel. Topics Power Electron., vol. 8, no. 2, pp. 1767–1781, Jun. 2020
- [14] J.Liu,Z.Zheng,K.WangandY.D.Li,"ComparisonofboostandLLCconverterandactiveclampisolatedfullbridgeboostconverterforphotovoltaicDCsystem",J.Eng.,vol. 2019,no.16,pp.3007-3011,Mar.2019.
- [15] M.Truntič,T.Konjedic,M.Milanovič,P.ŠlibarandM.Rodič,"Controlofintegratedsingle- phase PFC charger for EVs", IET Power Electron., vol. 11, no. 11, pp. 1804-1812, 2018.
- [16] A.K.SinghandM.K.Pathak,"Integratedconverterforplug-inelectricvehicleswithreduced sensor requirement", IET Elect. Syst. Transport., vol. 9, no. 2, pp. 75-85, 2019.
- [17] Y. Jang and M. M. Jovanovic, "Bridgeless high-power-factor buck converter", IEEE Trans. Power Electron., vol. 26, no. 2, pp. 602-611, Feb. 2011.



10.22214/IJRASET



45.98



IMPACT FACTOR:
7.129



IMPACT FACTOR:
7.429



INTERNATIONAL JOURNAL FOR RESEARCH

IN APPLIED SCIENCE & ENGINEERING TECHNOLOGY

Call : 08813907089  (24*7 Support on Whatsapp)